

Flavonoids Inhibit Heparin-Induced Aggregation of the Third Repeat (R3) of Microtubule-Binding Domain of Alzheimer's Tau Protein

Lin-Jie Han,[1] Shuo Shi,[1] Leng-Feng Zheng,[1] Dan-Jing Yang,[1] Tian-Ming Yao,*[1] and Liang-Nian Ji[1,2]

[1]Department of Chemistry, Tongji University, Shanghai 200092, P. R. China

[2]MOE Laboratory of Bioinorganic and Synthetic Chemistry, School of Chemistry and Chemical Engineering, Sun Yat-Sen University, Guangzhou 510275, P. R. China

Received September 24, 2009; E-mail: tmyao@tongji.edu.cn

The abnormal aggregation of tau protein into paired helical filaments (PHFs) is one of the hallmarks of Alzheimer's disease. Although some small molecules capable of inhibiting the aggregation have been discovered, knowledge of relevant mechanisms is fragmentary. In this paper, Alzheimer's tau fragment R3 corresponding to the third repeat of microtubule-binding domain was selected as the tau model. We, for the first time, reported flavonoids for their ability to inhibit heparin-induced assembly of R3 by thioflavin S (ThS) fluorescence assay. Moreover, we further proposed the possible inhibition mechanism of six flavonoid compounds, applying tyrosine fluorescence quenching and circular dichroism (CD) methods. It was shown that flavonoids could inhibit fibril formation of R3 by deformation of the flexible extended structure, consequently losing its aggregation ability. The inhibitory ability is closely related to their binding modes and binding degree to R3. Finally a specific flavonoid structure was found to play an important role in inhibition.

Alzheimer's disease (AD) is the most common cause of dementia in elderly population. It is characterized by two pathological protein deposits, senile plaques which are made up largely of β-amyloid peptide,[1] and neurofibrillary tangles which are bundles of paired helical filaments (PHF) of protein tau.[2] Tau is a neuronal microtubule-associated protein (MAP), and its important function is the stabilization of axonal microtubules.[3] It is highly soluble and rarely shows any tendency to assemble under physiological conditions. In the brains of AD patients, however, it dissociates from its natural partner, the microtubule, and aggregates to form insoluble fibers.[4] Therefore, one of the priorities in Alzheimer research is to develop a compound that is able to inhibit PHF formation by tau protein.

Recently several molecules capable of inhibiting aggregation of tau protein have been reported. Rhodanine, phenylthiazolylhydrazide, phenylamine, anthraquinone, benzothiazole, phenothiazine, and porphyrin have been considered to be inhibitors of tau aggregation as potential disease-modifying drugs for Alzheimer's disease and other tauopathies.[5] However, knowledge of the structure-based inhibitory mechanism is fragmentary and imperfect. Herein we first report the investigation of flavonoid with such property in vitro, and further explored the inhibitory mechanism and presumed specific structure necessary for the inhibition.

The flavonoids comprise an important group of naturally occurring bioactive polyphenolics, ubiquitous in plants of higher genera.[6] Recent interests on flavonoids have largely focused on their biological and relevant therapeutic applications. Their structure is characterized by a diphenylpropane (C6C3C6) skeleton, consisting of two aromatic rings (ring **a** and **b** in Figure 1) linked by an oxygen-containing heterocycle (ring **c**). The flavonoid family includes monomeric flavanoids, flavanones, anthocyanidins, flavones, and flavonols, and these compounds are found in almost every plant.[7] Consumption of plants and plant products that are rich in flavonoids, such as cocoa, wine, tea, and berries, has been related with protective effects against cardiovascular disease and certain forms of cancer.[8] They have been found to act as free-radical scavengers and have been widely studied for their antioxidant activity in vitro.[9,10] Several authors have observed that antioxidants exhibit protective effect in a family of neurodegenerative diseases featuring memory loss, inability to calculate, visual-spatial disturbances, confusion and disorientation, such as Parkinson's disease and Alzheimer's disease.[11,12]

Tau protein includes the microtubule-binding domain (MBD) composed of a three- or four-repeat structure (3RMBD or 4RMBD, respectively), where each repeat peptide (named R1 to R4, from the first unit to the forth unit) consists of 31 or 32 amino acid residues.[4] As the third repeat R3 (residues 306–336: VQIVY KPVDL SKVTS KCGSL GNIHH KPGGG Q, according to the longest tau peptide) has been found to play an essential role in tau aggregation induced by heparin,[13–15] it is reasonable to investigate the effect of inhibitors on tau filament formation by using R3 peptide.

In this paper, apigenin (**A**), catechin (**C**), daidzein (**D**), epicatechin (**E**), kaempferol (**K**), and luteolin (**L**) (Figure 1) were selected as representative of flavonoid in order to gain insight into their neuroprotective effects, as indicated in their ability to inhibit heparin-induced assembly of tau R3 peptides into filaments in vitro. To investigate the relationship between their chemical structures and inhibitory modes in greater detail, we explored the inhibitory behavior toward heparin-induced filament formation of R3 by thioflavin S (ThS) fluorescence, tyrosine fluorescence quenching of R3 by flavonoid as a quencher, and circular dichroism (CD) spectrum.

Published on the web July 24, 2010; doi:10.1246/bcsj.20090254

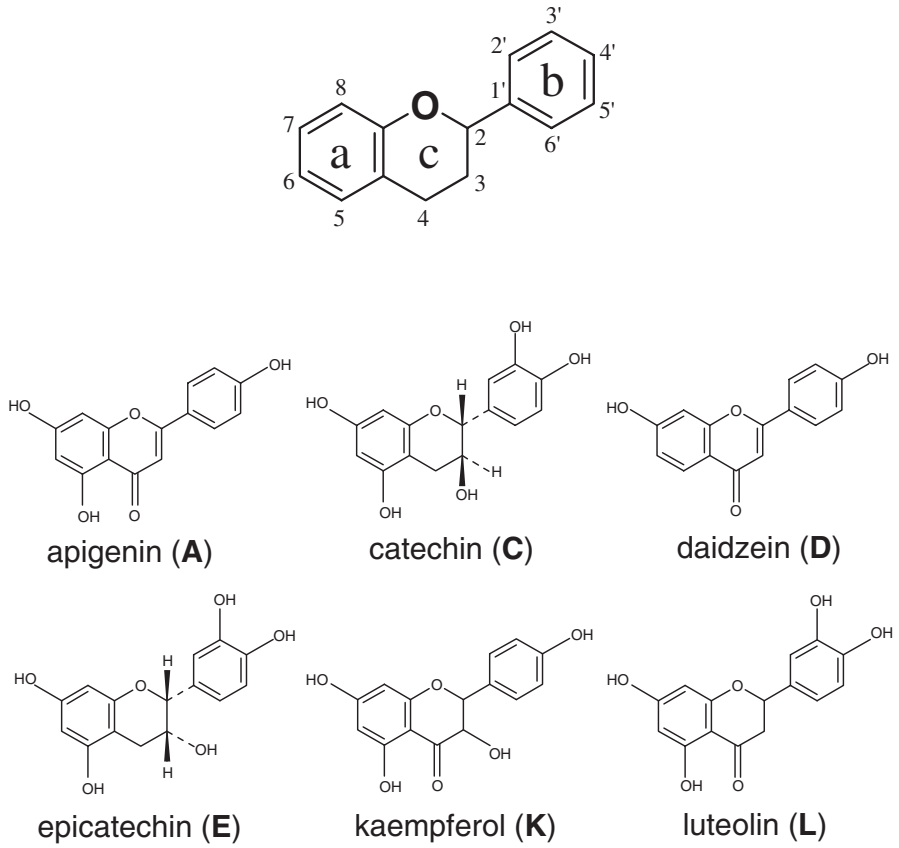

Figure 1. Basic structure and numbering system of flavonoids (upper) and structures of six selected flavonoids (lower).

Results

Kinetics of R3 Aggregation Measured Fluorimetrically. Thioflavin S (ThS) fluorescence was used to investigate the effects of flavonoids on the heparin-induced assembly of R3 into filaments. This method is based on the binding of ThS to fibers, which causes a change in the fluorescence spectrum.[16] Here we performed polymerization of R3 in the absence and presence of flavonoids.

It was important to note that the potential influence of heparin could be ruled out, when heparin here was used as a co-factor for inducing filament assembly. Taniguchi et al.[17] studied the binding of tau to heparin-Sepharose in the presence of inhibitory compounds. None of the compounds interfered with the binding of tau to heparin.

The impact of six flavonoids on the aggregation reaction of R3 was evaluated by ThS fluorescence assay. As illustrated in Figure 2 (Line blank), the time profile of ThS fluorescence of R3 aggregation induced by heparin showed the same pattern as reported earlier.[13] Addition of six different flavonoids into the solution impeded the increase of ThS fluorescence to a varying degree. This phenomenon indicated that all six flavonoids had inhibitory ability toward heparin-induced R3 aggregation. It also suggested that **L** has the strongest inhibitory ability among the six, and then **C**, **E**, **A**, **K**, and **D** in descending order.

Inhibition of R3 Filament Assembly Indicated by IC_{50} Values. Again based on the fluorescence change of the aggregate-specific stain ThS as a readout, we performed a R3 aggregation assay in vitro in order to determine the IC_{50} values

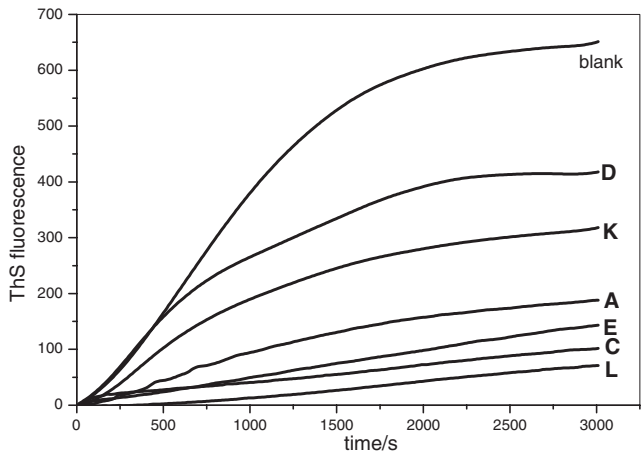

Figure 2. ThS fluorescence intensity vs. time profiles of heparin-induced filaments formation of R3 in the absence and presence of **A**, **C**, **D**, **E**, **K**, and **L** (15 μM) respectively in 50 mM Tris-HCl buffer (pH 7.5).

of those six different flavonoids, corresponding to the half maximal compound concentration necessary for their inhibition of R3 assembly into aggregates.

Inhibition of R3 filament formation was concentration-dependent, as illustrated in Figure 3 for flavonoids. The IC_{50} values of six different flavonoids for inhibiting R3 filament assembly are given in Table 1. A strong inhibitory effect on tau filament assembly (IC_{50} values of 26.8 μM) was observed with **L**. Weak inhibition (IC_{50} values of 109.8 and 150.28 μM,

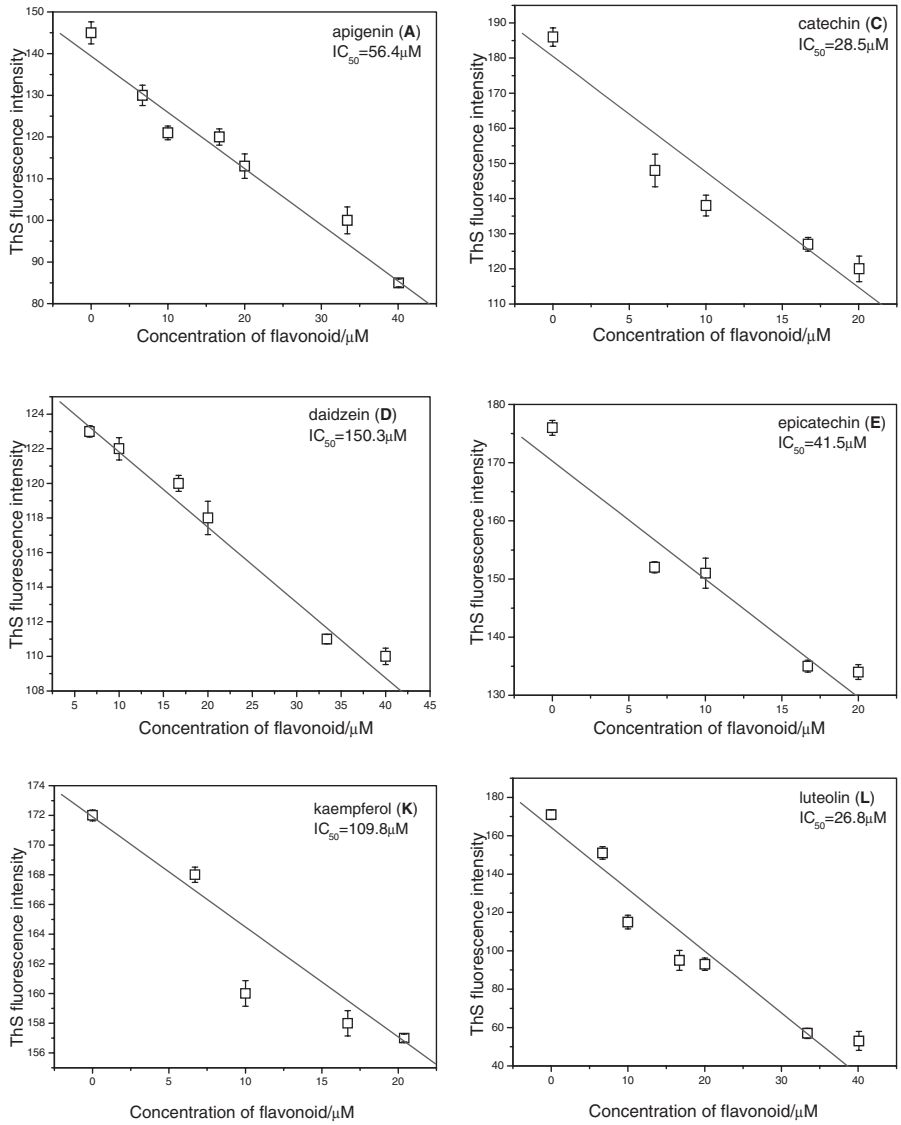

Figure 3. Concentration-dependent inhibition of R3 filament formation by six different flavonoids. Stock solution of R3 was diluted to a final concentration of 15 μM in 1000 μL of Tris-HCl buffer containing 3.8 μM heparin, in the presence or absence of flavonoid (concentration of 0, 5, 10, 15, 20, 30, and 40 μM). Following a 4 h incubation at 37 °C, 10 μM (final concentration) ThS was added. Fluorimetry was performed using a LS55 fluorescence spectrophotometer (set at 440 nm excitation/500 nm emission), and IC_{50} values were calculated for each compound.

Table 1. IC_{50} Values for R3 Assembly Inhibition

	Flavonoid					
	Apigenin (**A**)	Catechin (**C**)	Daidzein (**D**)	Epicatechin (**E**)	Kaempferol (**K**)	Luteolin (**L**)
IC_{50}/μM	56.4	28.5	150.3	41.5	109.8	26.8
r	0.9792	0.9492	0.9797	0.9689	0.9439	0.9595

respectively) was observed with **K** and **D**. This IC_{50} sequence is totally in agreement with the result described in the above section.

Conformational Conversion of R3 with and without Flavonoids. To ascertain the possible influence of flavonoid binding on the secondary structure of R3, we have performed CD studies in the presence of different concentrations of flavonoid. In Figure 4, CD spectra of R3 exhibited a strong negative band at 197–198 nm in the ultraviolet region, characteristic of a random coil structure of protein. It was revealed that the binding of flavonoid to R3 caused a decrease in band intensity at 197–198 nm in the far-ultraviolet region, without significant shift of the peaks. This change in CD spectrum clearly indicates that flavonoids result in a conformational alteration of R3 from random coil to other secondary structure, although we cannot identify which type it is, probably due to the low sensitivity of

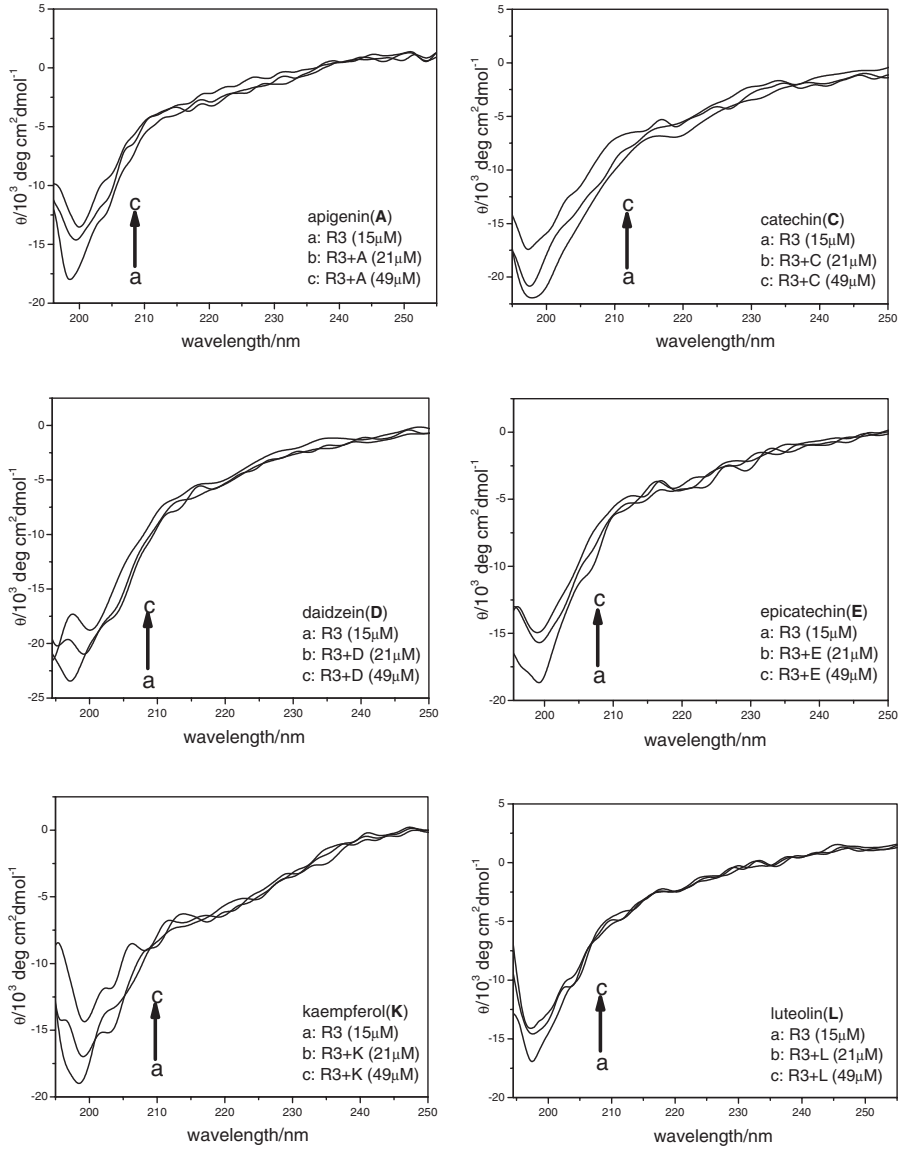

Figure 4. CD spectra of the R3–flavonoid system: (a) 15 μM R3, (b) 15 μM R3 + 21 μM flavonoid, and (c) 15 μM R3 + 49 μM flavonoid.

CD spectrum. The same phenomenon has also been observed in our early report,[18] and in the works of other groups.[19]

Fluorescence Quenching of R3 by Flavonoids. It has been known that in the ThS assay the dye has to bind to the filaments, which requires a minimal length of the fibers. The intrinsic fluorescence assay depends on the local surrounding of the fluorescent chromophore, the tyrosine residue of R3, and is therefore less dependent on the length of the filaments.[20]

Therefore the interaction of six different flavonoids with R3 was carried out by using the tyrosine fluorescence quenching at 307 nm at different temperatures (37 and 20 °C), as shown in Figure 5. In all cases, with the increasing of the concentration of flavonoid the fluorescence intensity of R3 gradually decreased, but with further addition of flavonoid the fluorescence decreased slowly which indicated the saturation of the R3 binding site. Additionally there was no apparent shift of the maximum $\lambda_{em} = 307$ nm.

Discussion

Inhibitory Ability of Flavonoids toward Heparin-Induced R3 Aggregation. A characteristic feature of brains afflicted with Alzheimer's disease is the abnormal deposition of two types of proteins, the amyloid peptide Aβ, and the microtubule-associated protein tau. Previous work has identified many substances that prevent β-sheet formation and the accompanying precipitation of β-peptide into amyloid, but there has been very little work on the inhibition of tau aggregation, not to mention that relatively few are known to inhibit it in a conformationally specific manner.

The purpose of the current study was to test flavonoids for their ability to inhibit the heparin-induced assembly of R3 (a very important fragment of tau) into filaments and their binding properties with R3, using fluorescence and CD spectroscopic techniques.

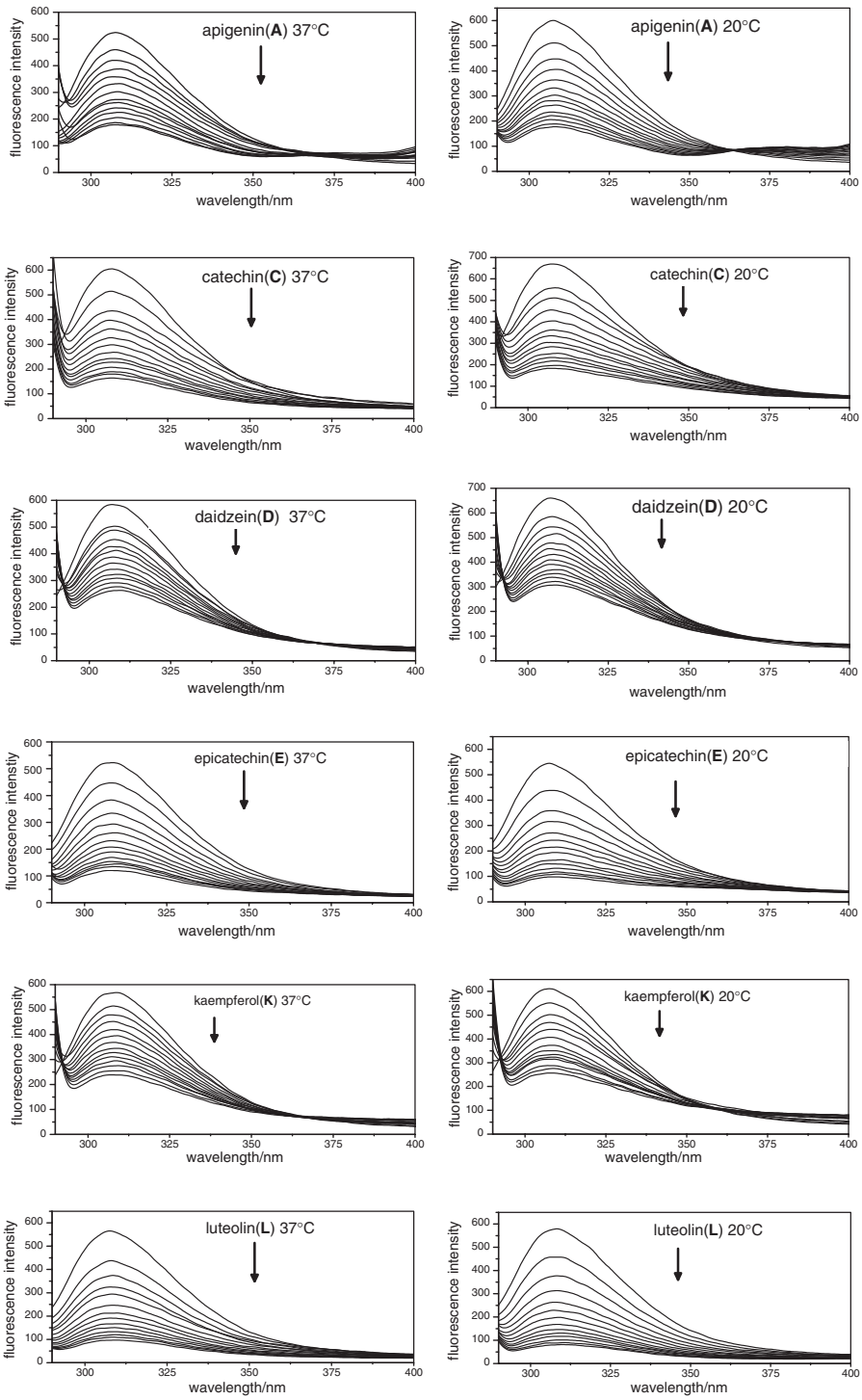

Figure 5. Emission spectra of R3 (25 μM) at $\lambda_{ex} = 275$ nm in the presence of different concentration of **A**, **C**, **D**, **E**, **K**, and **L**, at 37 and 20 °C respectively. Total concentration of flavonoid: (1) 3, (2) 6, (3) 9, (4) 12, (5) 15, (6) 18, (7) 21, (8) 24, (9) 27, (10) 30, (11) 33, (12) 36, and (13) 39 μM.

To investigate the effect of six flavonoids on the heparin-induced R3 aggregation, the ThS fluorescence was monitored as function of time in the absence and presence of six flavonoids. Consequently, it was clarified that **L** had the strongest inhibitory ability among the six, and then **C**, **E**, **A**, **K**, and **D** (from strong to weak). Similar results were also observed in the IC_{50} value analysis.

Possible Inhibition Mechanism. It has been known that all the six flavonoids inhibit the heparin-induced filament formation of R3 in a concentration-dependent manner, to a varying degree. Since they all share the flavone backbone (2-phenylchromone) (Figure 1), it may be concluded that such basic common structure plays a role in inhibition. However, two questions here need to be answered. (1) What is the possible

mechanism of the inhibitory effect by this conjugated system formed by ring **a**, **b**, and **c**? (2) Why do six flavonoids show varied inhibitory ability, since they all share the common basic structure?

To answer the first question, CD spectra were employed. The CD results have clearly demonstrated that the binding of all six flavonoids to R3 cause a partial elimination of the random coil structure of the protein. This may suggest that the freedom in rotation or folding of peptide chain gradually degenerated when the organic molecules bound to the peptide. It has been reported that the rigid extended structure of V(306)QIVYK(311) sequence at the N-terminal of R3 is important for facilitating aggregation.[21] In conjunction with the data of tyrosine fluorescent quenching experiments, the CD results may imply that the inhibition of filament formation by flavonoids is due to the deformation of the flexible extended structure most probably at the N-terminal of R3, consequently losing its aggregation ability as postulated by some earlier reports.[14,22]

For the six different flavonoid inhibitors, the changing trends of CD spectra were quite similar. The difference was unclear, although we attempted to identify the distinct impacts of the six flavonoids on the conformation of tau peptide. Therefore, to answer the second question why six flavonoids exhibited different inhibitory ability, additional physical method should be considered.

Type of Fluorescence Quenching (Stern–Volmer Plot). The interactions of R3 with six different flavonoids were then investigated by tyrosine fluorescence quenching. In general, the fluorescence lifetime of biomacromolecule is 10^{-8} s, and the maximum diffusion collision rate constant of various quenchers to biomacromolecule is $2.0 \times 10^{10}\,\mathrm{L\,mol^{-1}\,s^{-1}}$.[23] If the maximum diffusion collision rate constant is greater than $2.0 \times 10^{10}\,\mathrm{L\,mol^{-1}\,s^{-1}}$, the quenching process is static. Because static quenching refers to formation of a fluorophore–quencher complex, it would be possibly affected by temperature. Based on the above, the static and dynamic quenching can be distinguished according to the relationship of temperature and K_{SV}. If the value of K_{SV} at high temperature is greater than that at low temperature, the process should be dynamic quenching.

In order to judge the type of quenching, the procedure was first assumed to be dynamic quenching. Figure 6 shows the Stern–Volmer plots for the R3 fluorescence quenching by those six different flavonoids at 37 and 20 °C. Obviously, the Stern–Volmer plot has an upward curvature, concave toward the y axis. This characteristic feature means that the protein can be quenched by both mechanisms, or there exists a "sphere of action," indicating the apparent static quenching.

The linear Stern–Volmer plots (see Experimental section, eq 4) of R3 are also shown in Figure 6. In terms of the experimental data, the values of K_{SV} and K_q were calculated and listed in the Table 2. It can be seen that the values of K_q are far greater than $2.0 \times 10^{10}\,\mathrm{L\,mol^{-1}\,s^{-1}}$ and the values of K_{SV} at low temperature are larger than that at high temperature for flavonoids. This indicates that the fluorescence quenching of R3 in the presence of flavonoids was static, thus suggesting a binding site located near the internal tyrosine residue of R3.[24]

Binding Constant (Lineweaver–Burk Plot) and Number of Binding Site *n* (Scatchard Plot). Because of static quenching, the quenching constant was considered as indicative of the binding constant of flavonoid to R3. The Lineweaver–Burk double-reciprocal plot was made by $(F_0 - F)^{-1}$ versus $[Q]^{-1}$ (Figure 7) and K was listed in Table 3. The binding constant K of R3-flavonoid complexes calculated from the protein fluorescence quenching showed that the binding affinities of the six compounds decreased as follows: **L** > **E** > **C** > **A** > **K** > **D**.

The binding parameters can also be calculated using the Scatchard's procedure.[25] This method is based on the general equation:

$$r/D_f = nK - rK \tag{1}$$

where r ($r = \Delta F/F_0$) is the number of mol of bound drug per mol of protein, D_f is the concentration of unbound drug, K and n are the binding constant and number of binding sites.

In Table 3, the number of binding sites obtained from the Scatchard method (as shown in Figure 8) is listed for flavonoid associated with R3. The number of binding sites between R3 and **C**/**E** is less than 1 while it is more than 1 for the other four flavonoids.

Binding Affinity (van't Hoff Relationship). Essentially there are four types of noncovalent interactions that could play a role in ligand binding to proteins: hydrogen bonds, van der Waals forces, hydrophobic bonds, and electrostatic interactions.[26] To obtain such information, the implications of the present results have been discussed in conjunction with thermodynamic characteristics obtained for flavonoid binding, and the thermodynamic parameters were calculated from the van't Hoff plots.

If the temperature change is small, ΔH can be regarded as a constant.

$$\ln(K_2/K_1) = ((1/T_1) - (1/T_2))\Delta H/R \tag{2}$$

$$\Delta G = -RT\ln K = \Delta H - T\Delta S \tag{3}$$

From the above two thermodynamic equations, the values of enthalpy change ΔH, free energy change ΔG, and entropy change ΔS can be obtained (Table 4) using the experimental data. In this paper, the binding constants of K_1 and K_2 were obtained from the experimental results at 20 and 37 °C, respectively.

At a constant pressure and temperature, the sign of $\pm\Delta G$ shows whether a process occurs spontaneously or not. So the negative ΔG change here means that all six flavonoids can bind to R3 spontaneously.

Glatz[27] and Tian[28] have characterized the sign and magnitude of the thermodynamic parameter associated with various kinds of interaction that may take place in protein association processes, as described below. From the point of view of water structure, a positive ΔS value is frequently taken as typical evidence for hydrophobic interaction. Furthermore, specific electrostatic interactions between ionic species in aqueous solution are characterized by a positive value of ΔS and a negative ΔH value, while negative ΔS and ΔH changes arise from van der Waals forces and hydrogen formation in low dielectric media.

As illustrated in Table 4, the association between R3 and six flavonoids displays positive values of ΔS, indicating that hydrophobic forces exist mainly because of the nonpolar

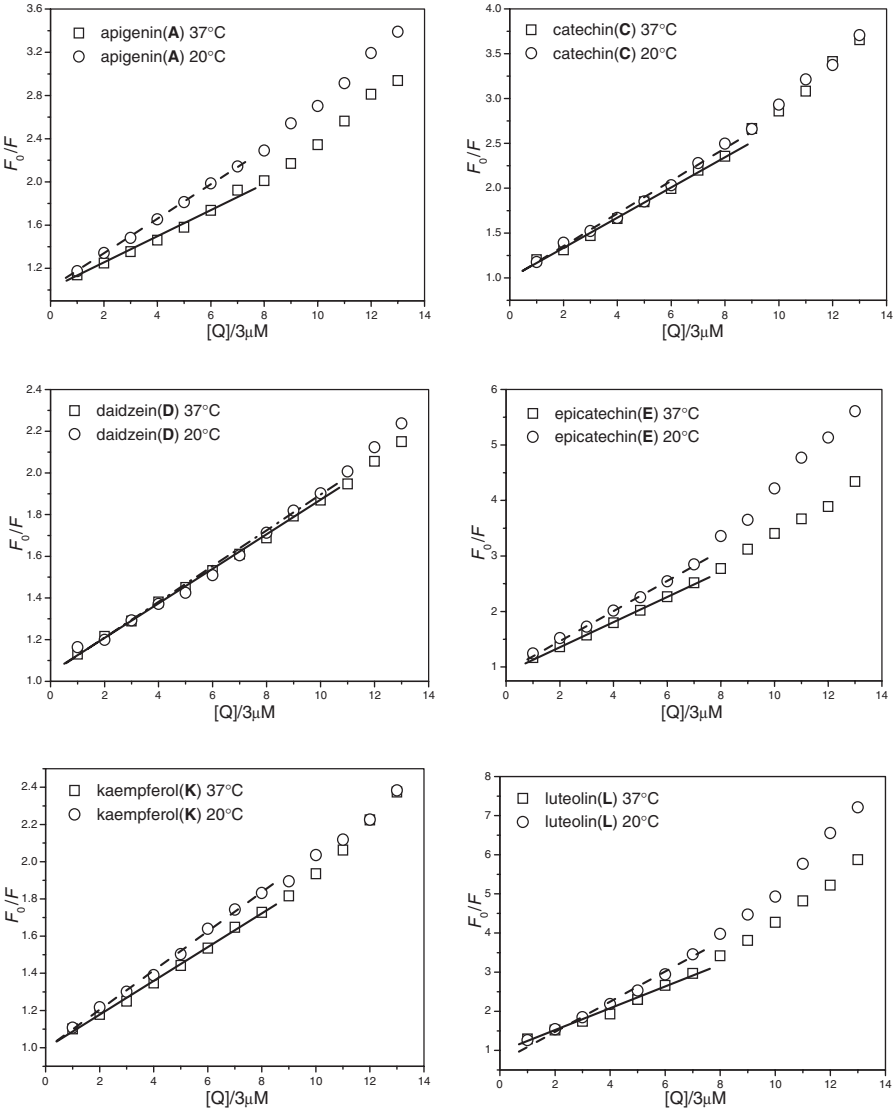

Figure 6. Stern–Volmer plot describing tyrosine quenching of R3 (25 μM) in the presence of different concentrations of **A**, **C**, **D**, **E**, **K**, and **L**, at 37 and 20 °C respectively. Fluorescence emission intensity was recorded at $\lambda_{ex} = 275$ nm, and the λ_{em} maximum occurred at 307 nm. The fitted linear regression curves represent the linear range at initial lower [Q].

Table 2. Stern–Volmer Dynamic Quenching Constants and Quenching Rate Constants of Six Flavonoids (**A**, **C**, **D**, **E**, **K**, and **L**) to R3 at Different Temperatures

Flavonoid	T /°C	K_{sv} /10^4 L mol^{-1}	K_q /10^{12} L mol^{-1} S^{-1}	r
Apigenin (**A**)	37	4.23	4.23	0.9933
	20	5.39	5.39	0.9997
Catechin (**C**)	37	5.66	5.66	0.9984
	20	6.11	6.11	0.9961
Daidzein (**D**)	37	2.72	2.72	0.9996
	20	2.87	2.87	0.9957
Epicatechin (**E**)	37	7.49	7.49	0.9991
	20	8.80	8.80	0.9990
Kaempferol (**K**)	37	3.04	3.04	0.9985
	20	3.50	3.50	0.9982
Luteolin (**L**)	37	9.36	9.36	0.9929
	20	11.99	11.99	0.9949

aromatic ring in six flavonoids, which may approach the hydrophobic region of R3. It can be estimated that the only tyrosine residue of R3 is in close proximity to the benzopyrone moiety of flavonoid suggesting the existence of hydrophobic interaction between them, which provides a good structural basis to explain the efficient fluorescence quenching of R3 emission in the presence of flavonoid. Specifically, the tyrosine residue with benzene ring can match that of the flavonoid in space in order to alter the conformation of the complex.

In addition, negative enthalpy change of these flavonoids in the Tris-HCl buffer shows that electrostatic forces also act as a main effect in the binding of R3 and flavonoids. In buffered solutions of pH 7.5, R3 (isoelectric point pI = 10) bear positive charge because of the ionization of amino acid residues. Meanwhile, Mabry[29] and Agrawal[30] reported that the most acidic phenolic OH groups of flavonoid are in the 3-, 7-, and 4′-positions, which are dissociated at physiological pH. This process is far from being complete and results in a mixture

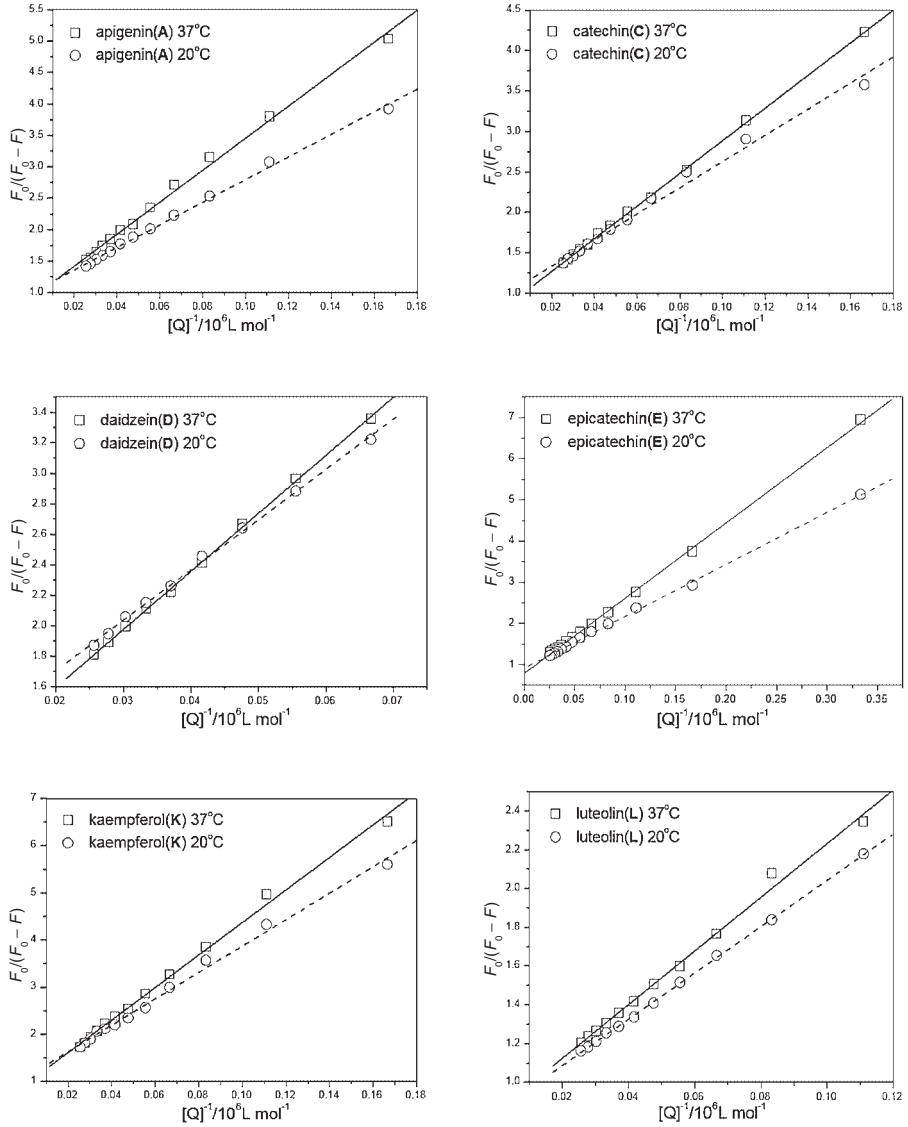

Figure 7. Double-reciprocal curves of fluorescence intensity with concentration of R3–flavonoid complex.

Table 3. Binding Parameters and Number of Binding Sites between R3 and Flavonoid at Different Temperatures

Flavonoid	T /°C	n	$r^{a)}$	K /10^4 L mol^{-1}	$r^{b)}$
Apigenin (**A**)	37	1.07	0.9711	3.93	0.9978
	20	1.19	0.9994	5.56	0.9984
Catechin (**C**)	37	0.71	0.9814	4.95	0.9997
	20	0.89	0.9950	6.18	0.9941
Daidzein (**D**)	37	1.27	0.9894	2.63	0.9996
	20	1.18	0.9781	3.03	0.9990
Epicatechin (**E**)	37	0.67	0.9837	5.47	0.9995
	20	0.67	0.9897	7.92	0.9993
Kaempferol (**K**)	37	1.21	0.9995	2.90	0.9980
	20	1.01	0.9975	3.57	0.9971
Luteolin (**L**)	37	1.11	0.9917	7.23	0.9971
	20	1.09	0.9870	8.38	0.9997

a) Correlation coefficient of regression for n value. b) Correlation coefficient of regression for K value.

of neutral and anionic species. In other words, flavonoid is partially negatively charged owing to the deprotonation of several hydroxy groups. In this regard, R3 and flavonoids are connected by electrostatic interaction.

However, the problem then exists as to which is the major force in the association. According to Gschwendt et al.,[31] if the enthalpic contribution to ΔG is more predominant, the ionic (charge neutralization) is the major force; if ΔG is primarily determined by positive entropy change rather than negative enthalpy change, the hydrophobic association constitutes the main binding force.

It is found that in the association between R3 and **D**, **K**, **L**, **A**, the major contribution to ΔG arises from the ΔS term rather than from ΔH, so the binding process is entropy driven. Thus, it can be deduced that the hydrophobic interaction might play a major role in the binding **D**, **K**, **L**, **A** to R3, which is consistent with an earlier report.[28] On the other hand, as for **E**–R3 and **C**–R3 systems, the main source of ΔG is derived from a relatively large contribution of ΔH term with less contribution from the

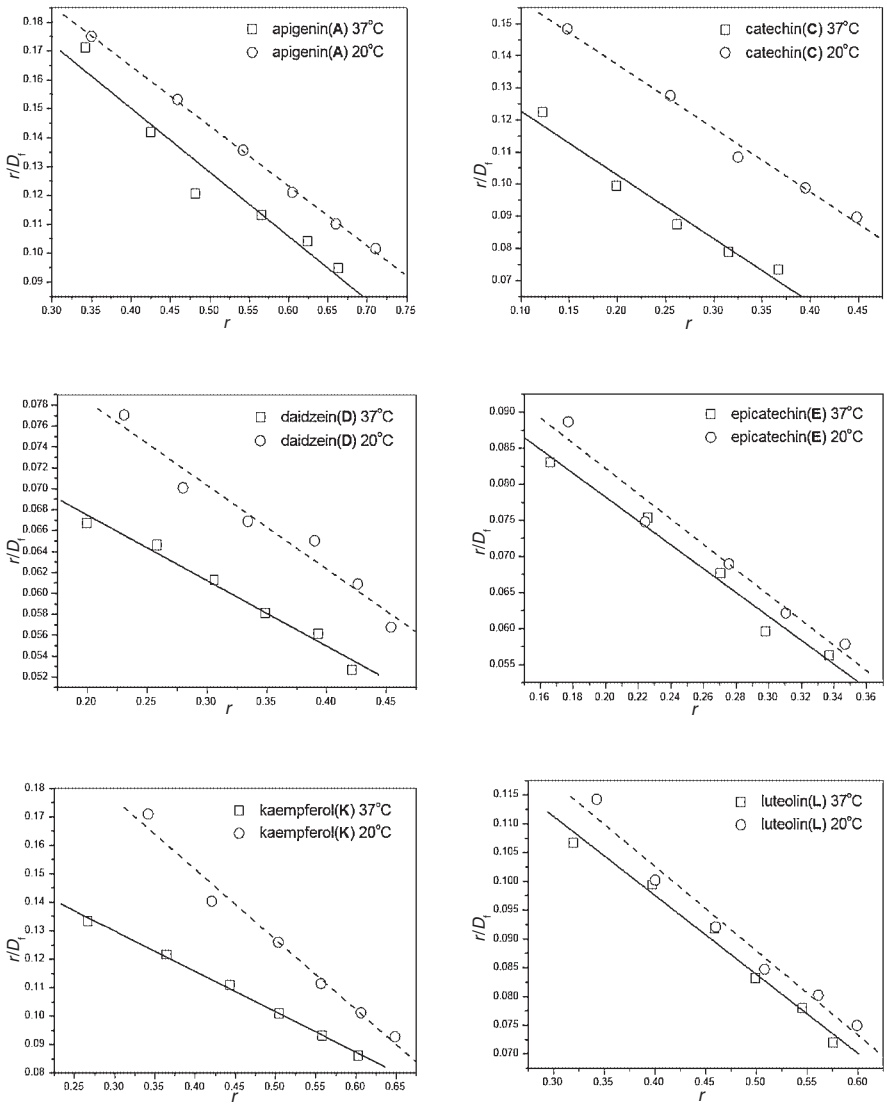

Figure 8. Scatchard plot for the flavonoid–R3 system at different temperatures obtained from the fluoremetric titration.

Table 4. Thermodynamic Parameters for the Interactions of Flavonoid and R3 at Different Temperatures

Flavonoid	T /°C	ΔG /kJ mol^{-1}	ΔH /kJ mol^{-1}	ΔS /J mol^{-1} K^{-1}	$-T\Delta S$ /kJ mol^{-1}
Apigenin (**A**)	37	−27.26	−8.45	60.67	−18.81
	20	−26.23	−8.45	60.67	−17.78
Catechin (**C**)	37	−27.67	−13.21	46.64	−14.46
	20	−26.87	−13.21	46.64	−13.66
Daidzein (**D**)	37	−26.22	−6.46	63.74	−19.76
	20	−25.13	−6.46	63.74	−18.67
Epicatechin (**E**)	37	−28.12	−16.44	37.68	−11.68
	20	−27.48	−16.44	37.68	−11.04
Kaempferol (**K**)	37	−26.48	−9.23	55.65	−17.25
	20	−25.54	−9.23	55.65	−16.31
Luteolin (**L**)	37	−28.84	−6.56	71.87	−22.28
	20	−27.61	−6.56	71.87	−21.05

ΔS factor, so the main interaction is electrostatic gravitation. This result is in good accordance with the papers by Kanakis[32] and Zsila.[33]

The reason for this is simple to explain. **E** and **C** contain more hydroxy groups than the other four flavonoids, as illustrated by slight solubility in cold water and relatively high solubility in hot water. Thus the additional stability of **E**/**C** and R3 can be assigned to the possible ionization of the ring OH group, which can interact with protein amino groups more effectively. So **E** and **C** show more tendencies to bind to R3 via electrostatic interaction.

As discussed above, the interaction between flavonoid and R3 is dominated by hydrophobic contacts or electrostatic force, but meanwhile there are also a number of hydrogen bonds. With flavonoid polyhydroxy compound, hydrogen bond is formed between the main chain carbonyl oxygen of R3 and phenolic hydroxy group of flavonoid. Therefore, it is clear that owing to the complexity of R3, many forces exist in the reaction between R3 and flavonoid. Hydrogen bonding, ionic, and hydrophobic interactions are important driving forces for R3–flavonoid association.

Binding Affinity and Structure of Flavonoid. It has been calculated that the binding affinities of the six compounds

decreased as follows: **L** > **E** > **C** > **A** > **K** > **D**. It was originally surmised that flavonoid containing more phenolic OH groups bound more strongly to R3, which meant the binding force might probably decrease as follows: **E**, **C** > **L**, **K** > **A** > **D**. However this is not the real case when compared with the above calculation. These facts suggest that the degree of binding affinity may be closely related to the position rather than the numbers of phenolic hydroxy groups.

Chen et al.[34] pointed out that the electron-withdrawing property of the chromonoid in ring **c** could increase O–H bond energy of hydroxy groups in ring **a** and make H dissociation difficult, whereas ring **b** weakly conjugated with ring **c** was less affected by this property. That is the reason why the scavenging activity of hydroxy groups in ring **b** is higher than that in ring **a**. So we suggested that –OH on the ring **b** (**b**-OH) were main active groups that promote the binding affinity between flavonoid and R3. Specifically speaking, the deprotonation of **b**-OH will result in the formation of hydrogen bonds and electrostatic interactions, further enhancing the binding of flavonoid to R3.

Binding Affinity and Inhibitory Ability. When relating the binding affinity between flavonoid and R3 (**L** > **E** > **C** > **A** > **K** > **D**) to their inhibitory ability (**L** > **C** > **E** > **A** > **K** > **D**), we can easily find that the more strongly flavonoid binds to R3, the greater inhibitory effect it has on the R3 aggregation. Salomon[35] once suggested that the inhibition of β-amyloid formation by nicotine might result from its binding to the more soluble α-helical structure of β-peptide. It is therefore conceivable that the inhibition of R3 assembly by flavonoid may be attributable to its powerful binding to R3, which in turn eliminates the flexible extended structure at the N-terminal of R3. So when compared with **A**, **D**, and **K** with only 3′-OH, **C**, **E**, and **L** with 3′-OH and 4′-OH can bind more strongly to R3, indicating stronger inhibitory ability.

Specific Structure of Flavonoid Important for Inhibitory Activity. Although **L**, **C**, and **E** possess the same amount of **b**-OH, the inhibiting effects of **E** and **C** were lower, when compared with **L**. Hence it is reasonable to assume that the planar anthocyanidin ring of **L** is important for inhibitory activity. Such planar aromatic ring can be coincidently accommodated in the small hydrophobic environment of R3, which was shown to be necessary for inhibition. The importance of the planar aromatic ring has also been reported by Hattori et al.[36] Another probable reason is that the basic moiety of **E** and **C** is not the complete 2-phenylchromone. It lacks the carbonyl group in ring **c**, thus negatively influencing the conjugated systems formed by ring **a**, **b**, and **c**, which is the basic factor for the inhibition, just mentioned above.

Conclusion

In conclusion, a number of flavonoids were shown to inhibit the aggregation of R3, to a different degree. They are inhibitory toward R3 filament assembly by virtue of their ability to bind to and partially eliminate the flexible extended structure of R3, consequently losing its aggregation ability. In addition, those retaining a high affinity for R3 show a relatively strong inhibitory ability for R3 aggregation. 2-Phenyl-1-benzopyran-4-one in flavonoid, namely conjugated systems formed by ring **a**, **b**, and **c**, is the basic structure for inhibition. When comparing the structures of more and less active flavonoid, we found that compounds with 3′-OH and 4′-OH were strongly inhibitory, whereas those with only 3′-OH weakly inhibitory. This observation outlines the importance of the –OH group at position 3′ and 4′ for the strong inhibitory ability. Finally, the planar aromatic ring of flavonoid was shown to be important for the inhibition.

Experimental

Chemicals. Heparin (average molecular weight, 6000) and ThS were obtained from Sigma Co. R3 was chemically synthesized using a solid-phase peptide synthesizer. The peptide was characterized by mass spectrometry and determined to be N95.0% pure by reverse-phase HPLC. The samples (including TFA as a counterion) were obtained in the lyophilized form. Working solution of R3 was made by dilution to 1 mg mL^{-1} with 50 mM Tris-HCl buffer (pH 7.50) before use. The buffer solution contained no reducing reagent such as dithiothreitol (DTT) usually used to block the formation of disulfide bonds. Flavonoids were purchased from Shanghai U-Sea Biotech Co and used as received without further purification. The flavonoid solutions (300 μM) were prepared in NaOH/Tris-HCl buffer mixture. All the experiments were conducted in open atmosphere. All the other chemicals were of analytical reagent grade.

Kinetics of R3 Aggregation Monitored by ThS Fluorescence. The concentration of R3 was adjusted to 15.0 μM using 50 mM Tris-HCl buffer (pH 7.5) containing 10 μM ThS dye. The aggregation was induced by adding (i) heparin (final concentration was 3.8 μM) and (ii) flavonoids (final concentration was 15.0 μM) and then heparin immediately (final concentration was 3.8 μM) to the solution and mixed with a pipette prior to fluorescence measurement. The time-dependent fluorescence at 37 °C was monitored on a LS-55 luminescence spectrometer instrument (Perkin-Elmer) with a 2 mm quartz cell with excitation at 440 nm and emission at 500 nm. The excitation and emission slit width were both 10 nm. The background fluorescence of the sample was subtracted when needed. For each curve of time-dependent ThS fluorescence, the measurement was performed three times and averaged.

IC_{50} Values for R3 Assembly Inhibition. Stock solution of R3 was diluted to a final concentration of 15 μM in 1000 μL Tris-HCl buffer containing 3.8 μM heparin, in the absence or presence of flavonoid (final concentration of 0, 5, 10, 15, 20, 30, and 40 μM) respectively, and incubated at 37 °C for 4 h. Then ThS (final concentration of 10 μM) was added to each solution, and fluorimetry was performed using a LS55 fluorescence spectrophotometer (set at 440 nm excitation/510 nm emission), and IC_{50} value was calculated for each compound.

CD Measurement. Solutions of 15 μM R3 in the absence or presence of flavonoids (21 and 49 μM) were prepared with 50 mM phosphate buffer (pH 7.5). All measurements were carried out at 25 °C with a JASCO J-810 spectrometer in a cuvette with a 10 mm path length. For each experiment, the measurement from 192 to 252 nm was repeated eight times under N_2 gas flow, and the results were summed. Then the molar ellipticity was determined after normalizing the sample concentration. The background of CD spectrum of R3 in presence of flavonoid (including the weak CD signal of

flavonoid containing chiral center) was subtracted by using a peptide-blank reference solution, a solution of flavonoid under the same condition, except for the absence of R3 peptide. The same experiment was performed at least three times using the newly prepared samples, and average values were presented in this paper.

Fluorescence Quenching Measurements. A Perkin-Elmer Model LS-55 luminescence spectrometer with a 2 mm quartz cell and a thermostat bath was used for fluorescence quenching measurements. The excitation wavelength was set at 275 nm, and the emission was recorded from 290 to 400 nm. Excitation/emission slit widths were set at 10 nm/10 nm.

For each data point, 5 μL of the appropriate flavonoid solution was added into 600 μL R3 solution (25 μM), to give a final flavonoid concentration in the range 3–39 μM. The change in fluorescence emission intensity was measured within 1 min of adding flavonoid to R3. The addition of a constant volume of quencher to the protein solution avoided complications due to dilution effects within titration experiments. Each measurement was repeated in triplicate.

Principles of Fluorescence Quenching. Fluorescence quenching is the decrease of the quantum yield of fluorescence from a fluorophore induced by a variety of molecular interactions with a quencher molecule. Fluorescence quenching acts an important tool to analyze the interaction between protein and quencher.

Fluorescence quenching can be static, resulting from the formation of a ground-state complex between the fluorophore and quencher, or dynamic, resulting from collisional encounters between the fluorophore and quencher.[37]

For the static quenching, the equation is described by Lineweaver–Burk plot:

$$(F_0 - F)^{-1} = {F_0}^{-1} + K^{-1}{F_0}^{-1}[\mathrm{Q}]^{-1} \quad (4)$$

Where F_0 and F are the fluorescence intensities before and after the addition of the quencher, respectively, [Q] is the concentration of the quencher, and K is the binding constant.

For the dynamic quenching, the equation is described by Stern–Volmer plot:

$$F_0/F = 1 + K_\mathrm{q}\tau_0[\mathrm{Q}] = 1 + K_\mathrm{sv}[\mathrm{Q}] \quad (5)$$

Where F_0, F, [Q] are the same as formerly, k_q is the bimolecular quenching constant, τ_0 is the lifetime of the fluorophore in the absence of quencher, and K_sv is the Stern–Volmer quenching constant. Hence, eq 5 was applied to determine K_sv by linear regression of a plot of F_0/F against [Q].

A linear Stern–Volmer plot is generally indicative of a single class of fluorophores in a protein, all equally accessible to the quencher; this also means that only one mechanism (dynamic or static) of quenching occurs. However, the Stern–Volmer plot sometimes exhibits an upward curvature, concave toward the y axis at high [Q]. This may be an indication of two distinct situations. In many cases, this upward curvature indicates that the fluorophore can be quenched by both collision and complex formation with the same quencher. In other cases, the upward curvature indicates the presence of a sphere of action. This assumes the existence of a sphere of volume around a fluorophore within which a quencher will cause quenching with a probability of unity. In this situation, quenching occurs due to the quencher being adjacent to the fluorophore at the moment of excitation. These closely spaced fluorophore–quencher pairs are immediately quenched, but fluorophores and quenchers do not actually form a ground-state complex. This type of apparent static quenching is usually interpreted in terms of the model "sphere of action."[38]

The authors thank the National Natural Science Foundation of China (No. 20871094, No. 20901060, and No. 20472065), the Research Fund for the Doctoral Program of Higher Education and the Program for Young Excellent Talents in Tongji University for their support of this research.

References

1 M. C. Montalto, G. Farrar, C. T. Hehir, *Ann. N. Y. Acad. Sci.* **2007**, *1097*, 239.
2 P. Friedhoff, M. von Bergen, E.-M. Mandelkow, P. Davies, E. Mandelkow, *Proc. Natl. Acad. Sci. U.S.A.* **1998**, *95*, 15712.
3 M. Goedert, R. Jakes, M. G. Spillantini, R. A. Crowther, in *Microtubules*, ed. by J. Hyams, C. Lloyd, Wiley-Liss, Inc., New York, **1994**, pp. 183–200.
4 P. Friedhoff, M. von Bergen, E.-M. Mandelkow, E. Mandelkow, *Biochim. Biophys. Acta* **2000**, *1502*, 122.
5 B. Bulic, M. Pickhardt, B. Schmidt, E.-M. Mandelkow, H. Waldmann, E. Mandelkow, *Angew. Chem., Int. Ed.* **2009**, *48*, 1740.
6 T. J. Mabry, K. R. Markham, M. B. Thomas, *The Systematic Identification of Flavonoids*, Springer-Verlag, New York, **1970**, p. 17.
7 L. Bravo, *Nutr. Rev.* **1998**, *56*, 317.
8 G. G. Duthie, S. J. Duthie, J. A. M. Kyle, *Nutr. Res. Rev.* **2000**, *13*, 79.
9 O. V. Brenna, E. Pagliarini, *J. Agric. Food Chem.* **2001**, *49*, 4841.
10 C. Counet, S. Collin, *J. Agric. Food Chem.* **2003**, *51*, 6816.
11 E. Esposito, D. Rotilio, V. Di Matteo, C. Di Giulio, M. Cacchio, S. Algeri, *Neurobiol. Aging* **2002**, *23*, 719.
12 A. V. Rao, B. Balachandran, *Nutr. Neurosci.* **2002**, *5*, 291.
13 K. Tomoo, T.-M. Yao, K. Minoura, S. Hiraoka, M. Sumida, T. Taniguchi, T. Ishida, *J. Biochem.* **2005**, *138*, 413.
14 S. Hiraoka, T.-M. Yao, K. Minoura, K. Tomoo, M. Sumida, T. Taniguchi, T. Ishida, *Biochem. Biophys. Res. Commun.* **2004**, *315*, 659.
15 T.-M. Yao, K. Tomoo, T. Ishida, H. Hasegawa, M. Sasaki, T. Taniguchi, *J. Biochem.* **2003**, *134*, 91.
16 P. Friedhoff, A. Schneider, E.-M. Mandelkow, E. Mandelkow, *Biochemistry* **1998**, *37*, 10223.
17 S. Taniguchi, N. Suzuki, M. Masuda, S. Hisanaga, T. Iwatsubo, M. Goedert, M. Hasegawa, *J. Biol. Chem.* **2005**, *280*, 7614.
18 L.-F. Jiang, T.-M. Yao, Z.-L. Zhu, C. Wang, L.-N. Ji, *Biochim. Biophys. Acta* **2007**, *1774*, 1414.
19 V. N. Uversky, J. Li, A. L. Fink, *J. Biol. Chem.* **2001**, *276*, 44284.
20 M. Pickhardt, Z. Gazova, M. von Bergen, I. Khlistunova, Y. Wang, A. Hascher, E.-M. Mandelkow, J. Biernat, E. Mandelkow, *J. Biol. Chem.* **2005**, *280*, 3628.
21 K. Minoura, T.-M. Yao, K. Tomoo, M. Sumida, M. Sasaki, T. Taniguchi, T. Ishida, *Eur. J. Biochem.* **2004**, *271*, 545.
22 K. Minoura, K. Tomoo, T. Ishida, H. Hasegawa, M. Sasaki, T. Taniguchi, *Bull. Chem. Soc. Jpn.* **2003**, *76*, 1617.

23 H. He, J. S. Yu, S. P. Xu, D. S. Zhou, Y. Liu, *Acta Pharmacol. Sin.* **2001**, *36*, 549.
24 W. He, Y. Li, C. Xue, Z. Hu, X. Chen, F. Sheng, *Bioorg. Med. Chem.* **2005**, *13*, 1837.
25 G. Scatchard, *Ann. N. Y. Acad. Sci.* **1949**, *51*, 660.
26 S. N. Timaseff, in *Protides of the Biological Fluids*, ed. by H. Peeters, Pergamon Press, Oxford, **1972**, pp. 511–519.
27 J. F. C. Glatz, J. H. Veerkamp, *J. Biochem. Biophys. Methods* **1983**, *8*, 57.
28 J. Tian, J. Liu, W. He, Z. Hu, X. Yao, X. Chen, *Biomacromolecules* **2004**, *5*, 1956.
29 T. J. Mabry, K. R. Markham, M. B. Thomas, *The Systematic Identification of Flavonoids*, Springer-Verlag, New York, **1970**, p. 354.
30 P. K. Agrawal, H. J. Schneider, *Tetrahedron Lett.* **1983**, *24*, 177.
31 M. Gschwendt, F. Horn, W. Kittstein, G. Fürstenberger, E. Basenfeklder, F. Marks, *Biochem. Biophys. Res. Commun.* **1984**, *124*, 63.
32 C. D. Kanakis, P. A. Tarantilis, M. G. Polissiou, S. Diamantoglou, H. A. Tajmir-Riahi, *J. Mol. Struct.* **2006**, *798*, 69.
33 F. Zsila, Z. Bikádi, M. Simonyi, *Biochem. Pharmacol.* **2003**, *65*, 447.
34 J. W. Chen, Z. Q. Zhu, T. X. Hu, D. Y. Zhu, *Acta Pharmacol. Sin.* **2004**, *23*, 667.
35 A. R. Salomon, K. J. Marcinowski, R. P. Friedland, M. G. Zagorski, *Biochemistry* **1996**, *35*, 13568.
36 M. Hattori, E. Sugino, K. Minoura, Y. In, M. Sumida, T. Taniguchi, K. Tomoo, T. Ishida, *Biochem. Biophys. Res. Commun.* **2008**, *374*, 158.
37 J. R. Lakowicz, *Principles of Fluorescence Spectroscopy*, 2nd ed., Kluwer Academic/Plenum Publishers, **1999**, p. 698.
38 S. Soares, N. Mateus, V. de Freitas, *J. Agric. Food Chem.* **2007**, *55*, 6726.